ORIGINAL PAPER

Theoretical study of glyphosate adsorption potential on methylcellulose and cellulose xanthate matrices compared to activated carbon: role of biopolymers in the adsorption process

Sílvio Quintino de Aguiar Filho[1] · Anna Karla dos Santos Pereira[2] · Grasiele Soares Cavallini[1] · Douglas Henrique Pereira[1]

Abstract

This study provides theoretical insights into the potential use of cellulose derivatives, such as methylcellulose (ME) and cellulose xanthate (CX), to remove glyphosate (GLY) contaminants via adsorption. The mechanism of adsorption in ME and CX is compared with that of activated carbon. To this end, theoretical calculations based on density functional theory (DFT) were used to determine the frontier molecular orbitals (FMOs); molecular electrostatic potential (MEP); and energetic, structural, and topological parameters. The analyses of FMOs and MEP indicated two possible interaction sites. The structural parameters showed that the herbicide interacts with the ME and CX matrices, and the bond lengths of the interaction ranging from 1.58 to 3.09 Å, depending on the nature of the interaction. The vibrational frequencies of the bonds involved in the interaction changed after adsorption, thus confirming the existence of the interaction. The analysis of the quantum theory of atoms in molecules (QTAIM) allowed the characterization of interactions through topological parameters and showed that the most effective interactions presented a higher number of electrostatic interactions. The determined energies of the electronic interaction and the enthalpy were negative, indicating that the interaction occurred. Finally, the calculations for the glyphosate adsorption process on activated carbon (AC) showed that the terminal group –COOH presented the best energy values for interaction with GLY, followed by activated carbon with the group –OH, and finally, the activated carbon containing only aromatic rings. The results showed that the derivatives of cellulose CX and ME are promising alternatives to remove glyphosate contaminants from water.

Keywords Activated carbon · Biopolymers · Adsorption · DFT

✉ Douglas Henrique Pereira
    doug@uft.edu.br

Extended author information available on the last page of the article

Introduction

Glyphosate, or *N*-(phosphonomethyl) glycine, is an organophosphate herbicide introduced to the market in 1974 under the formulation of glyphosate with adjuvant agents and other reagents of chemical composition with unpublished concentrations [1–4]. Glyphosate, both in pure and acid forms, is a white, odorless crystal [5].

The use of the glyphosate herbicide extends to more than 130 countries, with an estimated annual usage of 600 kilotonnes [6]. The extent of its use is justified by its wide spectrum of applications, which makes glyphosate effective in combating several weeds [6]. The use of genetically modified crops is another factor stimulating the use of herbicides as it may be required before and during the growth of the crops, and during the harvest [4]. Owing to the widespread and large-scale use of the herbicide glyphosate, concerns regarding environmental safety are rapidly increasing as glyphosate is a risk to ecosystem biodiversity and human health [4].

Glyphosate can have negative impacts on aquatic organisms at different trophic levels, such as protozoa, algae, plankton, mussels, crustaceans, frogs, and fish [7, 8], thereby changing the ecological balance. In terrestrial living beings, these impacts relate to population losses of various species of birds, mammals, and beneficial insects through habitat and/or supply destruction [7, 8]. Concerning humans, the *International Agency for Research on Cancer* (IARC) and a series of studies in the literature have related glyphosate to some form of cancer, attributing genotoxicity and mutagenicity to it [9–13].

In view of this growing problem, studies on methods to remove this herbicide from the environment have become increasingly crucial. These studies propose technologies for wastewater treatment by efficient and economically viable methods, such as adsorption [14–17].

Activated carbon is among the most widespread adsorbents; however, there is an ongoing search for more economical alternative materials [18, 19]. Some adequate candidates found in the literature are the following: zeolites and clays [20, 21], solid agricultural waste [22, 23], and industrial by-products [24].

One way to facilitate the search is to use theoretical calculations as a tool for selecting materials with significant adsorptive potential, which can either be used in conjunction with experimental results [20] or evaluated in advance to predict or simulate the possible adsorption mechanisms [25–28]. In this context, theoretical calculations are employed to analyze the adsorption process in molecular or electronic terms, evaluate the best adsorbent for a given adsorbate, and reduce the experimental costs and time [25, 28].

In this study, theoretical calculations were used to predict the adsorption potential of methylcellulose (ME) and cellulose xanthate (CX) derivatives with respect to glyphosate adsorbate. Additional simulations using the activated carbon adsorbent allowed a more pragmatic overview of the results because it compared a recently studied biomass with a consolidated adsorbent. In addition, the study describes information on these matrices at a molecular level, thus contributing to the understanding of the relevant chemical characteristics of these biopolymers.

Computational methods

Methylcellulose (ME), cellulose xanthate (CX), activated carbon, and glyphosate molecules were optimized to the minimum energy using density functional theory (DFT) [29–32] at the wB97XD/6–31+G(d,p) [33–36] level. The continuous solvent model SMD [37] was used to simulate the effects of water as a solvent.

The frontier molecular orbitals HOMO and LUMO and the molecular electrostatic potential (MEP) were generated with 0.02 isovalue and *density* 0.001 μa, respectively.

The interactions between adsorbents and adsorbates were calculated at the same level of theory. The energy parameters, electronic interaction energy, Gibbs energy (ΔG), and enthalpy (ΔH), were determined using Eq. (1).

$$\Delta X = X_{\text{complex}} - \left[X_{\text{adsorbent}} + X_{\text{adsorbate}} \right] \qquad (1)$$

where X is the sum of the electronic energies with the zero-point energy (E+ZPE) or Gibbs energy or enthalpy.

No imaginary frequency was found in the adsorption processes or for individual species, confirming their minimum energy. Some structures were designed using the GaussView program [38], and all calculations were performed using the Gaussian09 program [39].

Topological analyses were performed using the quantum theory of atoms in molecules (QTAIM) [40, 41–43] with the aid of the AIMALL package [44].

Results and discussion

The ME and CX matrices were studied using three monomeric units. Hydrogen atoms were added to the ends of the cut. This methodology was previously employed by other authors [25, 26] to obtain a lower computational cost and reduce the loss of the original properties of ME and CX as much as possible. The contra-ion (Na^+) was not considered for the CX matrix, simulating the experimental conditions.

Figure 1 shows the structural representations of the ME, CX biopolymers, and glyphosate (GLY).

Analysis of possible interaction sites

MEP and frontier molecular orbital (FMO) analyses were performed for ME and CX matrices to determine the possible complexation sites.

Figure 2 shows the MEPs of ME (Fig. 3a) and CX (Fig. 3b). The description of MEP is made from the present staining, in which blue regions represent electron-deficient sites with a density of positive charges and electrophilic activity. In contrast, the molecular regions with reddish/orange coloration are electron-rich regions with negative charge density and nucleophilic activity.

From the results, it can be inferred that the ME matrix contains regions with significant electronic density located in the hydroxyl (–OH) groups of the
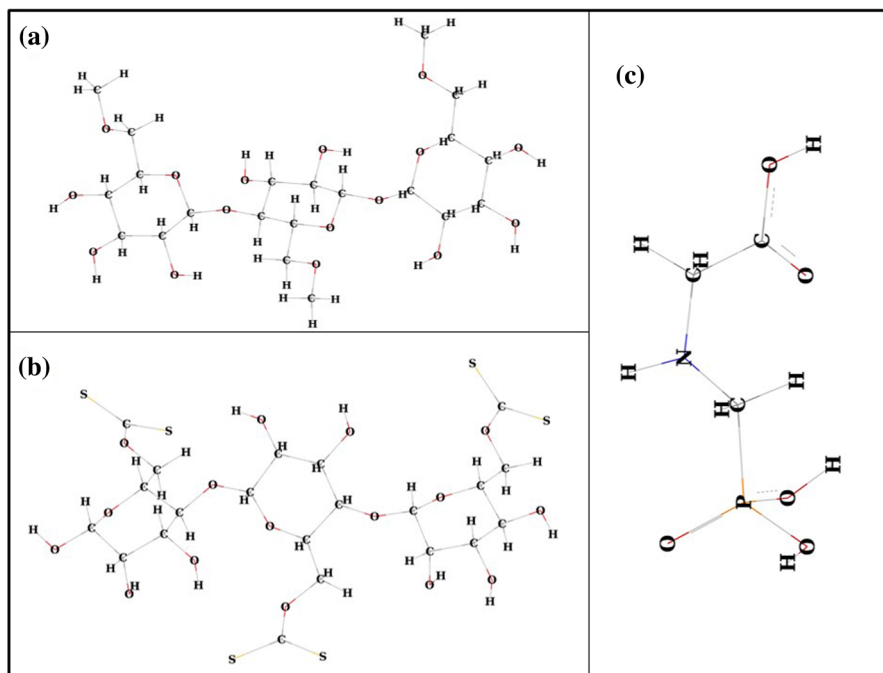
Fig. 1 Structural representation: **a** methylcellulose, **b** cellulose xanthate and **c** glyphosate
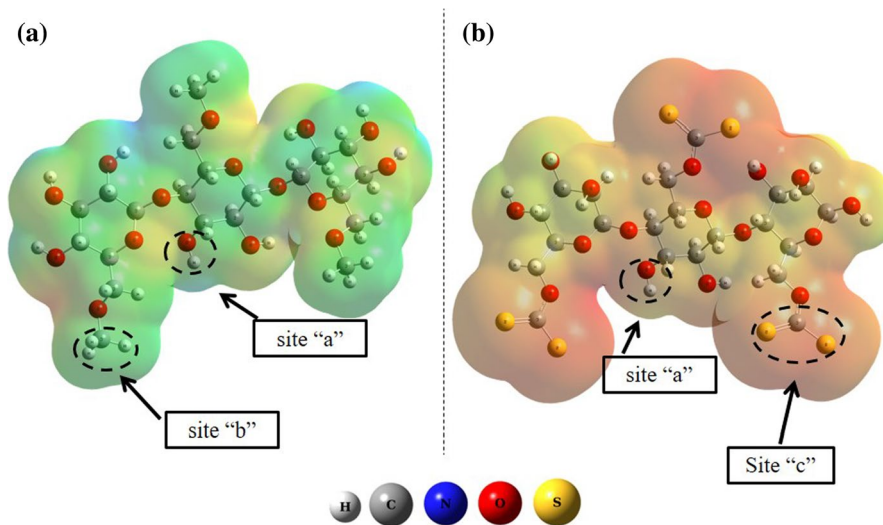

Fig. 2 Molecular electrostatic potential of methylcellulose (**a**) and cellulose xanthate (**b**)
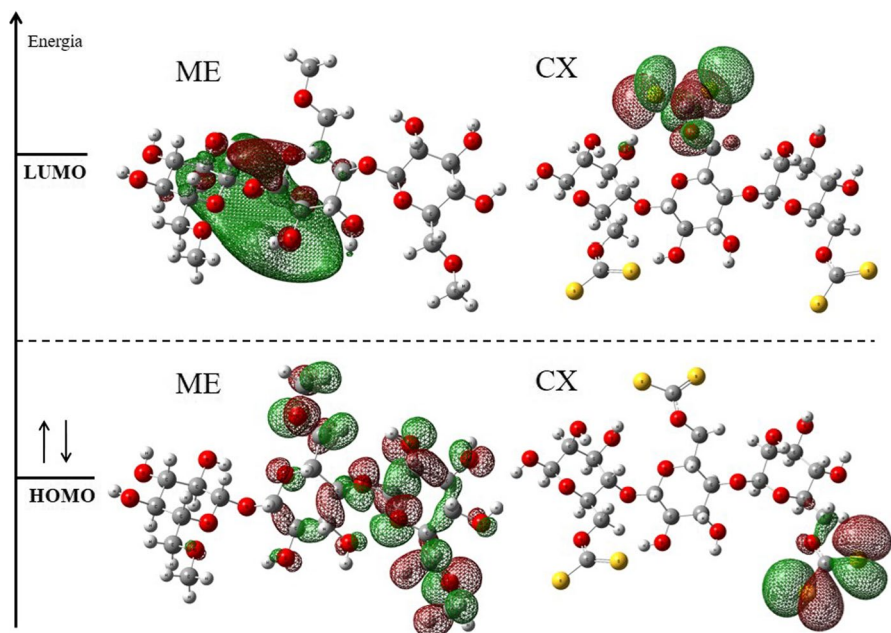
Fig. 3 Representation of HOMO and LUMO of ME and CX matrices

extremities. The methyl groups (–CH$_3$) were green and partially positive. Figure 2a represents the possible interaction sites, where sites "a" and "b" correspond to the –OH and –CH$_3$ groups, respectively.

The MEP for the CX shows that the whole structure consists of negative charge, originating from the –CS$_2^-$ groups. As indicated in Fig. 2b, two possible regions may interact with positive charges of other molecules as represented by the "a" and "c" sites of groups –OH and –CS$_2^-$, respectively.

In the literature, theoretical studies show that the glyphosate molecules and derivatives have negative charges concentrated around oxygen, positive charges in hydrogens, and the most stable conformation corresponds to the gg$^-$ arrangement [45, 46–48]. The results for GLY corroborate those presented in the literature [47] and were not reported in this work.

In addition to the MEPs, the analysis of FMO was used, both of which provide evidence of the probable interaction sites from the HOMO and LUMO.

Figure 3 shows the HOMO and LUMO of the ME and CX matrices, where ME presents a LUMO that extends along with two of its rings, while the HOMO has well-defined π orbitals in the central ring and ring on the right. The CX showed orbital π LUMO and π HOMO in the CS$_2^-$. This indicates that the main site of interaction in the CX matrix is in the CS$_2^-$ group.

It is important to highlight that the adsorbate in the adsorption process is initially in a liquid medium with a high degree of freedom and may interact with the frontier orbitals. In this context, two complexation hypotheses were evaluated for

each biopolymer, considering the FMOs and MEPs ((ME-GLY[1] and ME-GLY[2]) and (CX-GLY[1] and CX-GLY[2])).

Analysis of structural, energetic, and topological parameters post-complexation

Post-complexation studies: structural, energetic, and topological parameters were obtained from studies of possible sites in pre-complexation.

Structural parameters

Figure 4 shows the complexes formed after complexation, the values of the interaction distances between ME and GLY (ME-GLY[1] and ME-GLY[2]; Fig. 4a and b, respectively), and the complexes formed between CX and GLY (CX-GLY[1] and CX-GLY[2]; Fig. 4c and d, respectively).

The values of the bond lengths for the interactions are shown in Fig. 4, where "*a*," "*b*," and "*c*" represent the sites of interaction with the hydroxyls, methyl group, CS_2^- groups, respectively; "*x*" represents the interaction of GLY hydrogens with the oxygen of the ring. The ME-GLY[1] complex presented three interactions between hydrogen and –OH (a_1–a_3) group: two with the ring (x_1, x_2), and one with the group –CH_3 (b_1); whereas, the ME-GLY[2] complex presented only three interactions, two with –OH (a_4, a_5) and one with –CH_3 (b_2). The values of the interaction distances in "a" are less than the distances in "b".

The CX-GLY[1] complex has three interactions, two with –OH (a_6, a_7) and one with the sulfur and hydrogen atoms (c_1). The XC-GLI[2] complex has four interactions, two between hydrogen atoms and –OH (a_8 and a_9), and two between the sulfur atom and the hydrogen atom of GLY (c_2 and c_3). The values of the interaction bond lengths were lower for the CX-GLY[2] complex.

It is important to emphasize that the vibrational frequencies of the bonds of the functional groups that interact during the adsorption process changed after complexation, confirming that the interaction has occurred.

QTAIM analysis

The QTAIM analysis was used to determine the topological parameters: electronic density ($\rho(r)$), Laplacian of electronic density ($\nabla^2\rho(r)$), density of kinetic energy ($G(r)$), density of potential energy ($V(r)$), and density of potential energy in BCP ($H(r) = G(r) + V(r)$). The results of these interactions are presented in Table 1.

The electronic density values show that the most effective interactions (> 20 kcal mol^{-1}) are a_1, x_1, and x_2 for ME-GLY[1], a_4 and a_5 for ME-GLY[2], a_7 and c_1 for CX-GLY[1], and a_8 and c_2 for CX-GLY[2] (Table 1). The values of the Laplacian of the electronic density for the interactions are all higher than zero ($\nabla^2\rho(r) > 0$), indicating non-covalent interactions.
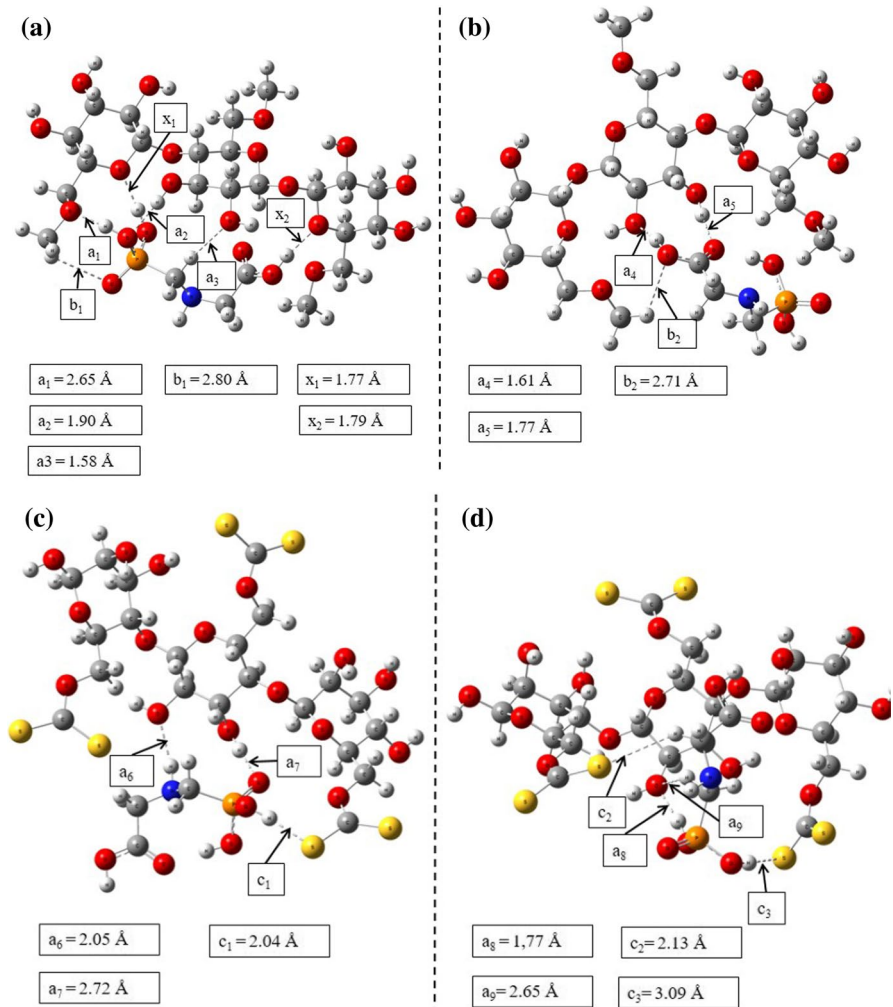
Fig. 4 Representation of complexes formed between ME and CX matrices with GLY and their respective interaction distances in **a** ME-GLY[1], **b** ME-GLY[2], **c** CX-GLY[1], and **d** CX-GLY[2]

One way to classify the interactions is through the parameters $\nabla^2\rho(r)$ and $H(r)$, in which partially covalent interactions are characterized by $\nabla^2\rho(r)>0$ and $H(r)<0$; and $\nabla^2\rho(r)>0$ and $H(r)>0$ are electrostatic. The results show that the interactions a_1, a_2, a_4, a_6, c_1, and c_2 are partially covalent, while the others correspond to electrostatic interactions.

From analyzing each complex separately, it can be observed that for ME-GLY[1], ME-GLY[2], and CX-GLY[2], there are more electrostatic interactions than partially covalent interactions. In contrast, the CX-GLY[1] complex showed two interactions, partially covalent and one electrostatic. Thus, electrostatic interactions are the interactions responsible for the adsorption process in almost all the evaluated sites.

Table 1 Topological parameters calculated in the BCPs of the interactions

Complex	Interaction (BCP)	$\rho(r)$ kcal mol^{-1}	$\nabla^2\rho(r)$	$V(r)$	$G(r)$	$H(r)$	Type of interaction
ME-GLY[1]	a_1 (O_{57}–H_{92})	38.19	98.89	−33.19	28.96	−4.24	Partially covalent
	a_2 (O_{91}–H_{47})	17.00	50.15	−12.86	12.70	−0.16	Partially covalent
	a_3 (O_{48}–H_{87})	5.49	18.24	−3.73	4.15	0.41	Electrostatic
	b_1 (O_{93}–H_{72})	3.59	12.68	−2.06	2.61	0.56	Electrostatic
	x_1 (O_{93}–H_{72})	20.74	65.25	−15.13	15.72	0.59	Electrostatic
	x_2 (O_{93}–H_{72})	21.69	68.42	−16.05	16.58	0.53	Electrostatic
ME-GLY[2]	a_4 (O_{48}–H_{82})	34.00	96.19	−27.87	25.96	−1.91	Partially covalent
	a_5 (O_{80}–H_{47})	22.50	73.10	−17.08	17.68	0.60	Electrostatic
	b_2 (O_{81}–H_{64})	4.05	15.28	−2.61	3.21	0.61	Electrostatic
CX-GLY[1]	a_6 (O_{53}–H_{81})	13.12	39.28	−10.45	10.14	−0.32	Partially covalent
	a_7 (O_{90}–H_{52})	25.46	79.99	−19.64	19.82	0.18	Electrostatic
	c_1 (S_{70}–H_{89})	26.22	32.34	−16.35	12.22	−4.13	Partially covalent
CX-GLY[2]	a_8 (O_{53}–H_{89})	27.88	86.79	−21.43	21.56	0.13	Electrostatic
	a_9 (O_{53}–H_{83})	6.28	21.18	−4.45	4.88	0.42	Electrostatic
	c_2 (S_{70}–H_{87})	20.45	31.46	−12.37	10.12	−2.25	Partially covalent
	c_3 (S_{24}–H_{76})	2.93	9.68	−1.23	1.82	0.59	Electrostatic

Table 2 Electronic interaction energy (ΔE_{int}) at 0 K, enthalpy (ΔH), Gibbs energy (ΔG) at 298 K, and variation of energy GAP (ΔGap) for the interaction of GLY with the ME and CX matrices

Complex	ΔE_{int} kcal mol^{-1}	ΔH	ΔG	ΔGap (%)
ME-GLY[1]	−22.79	−24.16	−3.56	4.06
ME-GLY[2]	−12.68	−14.26	6.25	0.16
CX-GLY[1]	−16.72	−17.84	0.41	22.64
CX-GLY[2]	−19.45	−20.74	−0.73	22.93

Energy parameters

The energy of electronic interaction (ΔE_{int}), enthalpy (ΔH), Gibbs energy (ΔG), and variation of the energy gap (ΔGap) involved in the interactions between the adsorbent and adsorbate were obtained (Table 2). The obtained energy values were used to analyze the magnitude of the interactions, heat released or absorbed, spontaneity, and its effects on the frontier orbitals after the interactions.

Table 2 shows that the interaction of ME-GLY[1] and CX-GLY[2] were the most significant interactions with interaction energy values of −22.79 and −19.45 kcal mol^{-1}, respectively, both having $\Delta G < 0$. All ΔH values are negative, showing that the process releases energy. ΔGap values demonstrate that the matrices most affected by adsorption were the CX matrices with a change in the ΔGap higher than 22%.

As evidenced by Costa et al. 2021 [49], in the study of the interaction of metal ions Hg^{2+} and Pb^{2+} on carboxymethyl diethylaminoethyl cellulose and cellulose nitrate matrices, the solvent effect significantly decreases the value of the interaction energy. In this context, only the implicit solvent effect was used in this work.

It is important to highlight that glyphosate speciation in water is relevant for the interaction process. The pK_a values for GLY are pKa1 = 2.0, pKa2 = 2.6, pKa3 = 5.6, and pKa4 = 10.6; therefore, there is a pH range between 2 and 11 according to the pKa of the groups present in the molecule [50]. For this study, a pH of 7 was studied (neutral molecule). For the ME matrix, the neutral molecule was also considered, and for the CX matrix, the anionic molecule was used because the sodium atom (Na) in water is transferred to the medium [51, 52].

Comparing the interaction energy values (Table 2) with the values found for the types of interactions (Table 1), it can be inferred that the ME-GLY^2 and CX-GLY^1 interactions are less favored because they have fewer electrostatic interactions.

Activated carbon and GLY

The ME and CX matrices are excellent alternatives for use in adsorptive processes to remove GLY contaminants. In this context, calculations of the adsorption potential of GLY with activated carbon were also performed.

For activated carbon, three types of adsorbents were evaluated: adsorbent composed of (i) only aromatic rings, (ii) aromatic rings with carboxylic groups (–COOH), and iii) aromatic rings with a hydroxyl group (–OH). The adsorbents and adsorption sites were built based on the work of Melchor-Rodríguez et al. (2020) [53]. Many functional groups can be found in activated carbon, and their structures change with changing pH. For this study, only carboxylic and hydroxyl groups were evaluated, and neutral molecules were considered (pH = 7). The results of AC-GLY optimized complexes (activated carbon-glyphosate) are shown in Fig. 5, with their respective bond lengths for the interactions.

The values of the interaction bond lengths range from 1.74 to 2.96 Å, depending on the interaction. The activated carbon with the –COOH group showed the shortest bond length (1.74 Å).

The energy of the electronic interaction and the thermodynamic properties of these interactions were also evaluated for activated carbon, and the results are presented in Table 3. From the results, it can be observed that the AC with the terminal group –COOH presented the best energy values for interaction with GLY, followed by AC with the group –OH, and finally the AC containing only the aromatic rings. For interactions with AC, it is necessary to emphasize that many factors can influence the adsorptive process, such as surface area, porosity, pH, and functional groups.

Another point to be highlighted is that studies in the literature suggest the use of biopolymers such as chitosan, chitin, and chitosan combined with alginate for glyphosate removal [54–58], and thus, theoretical studies provide insights for experimental verification.
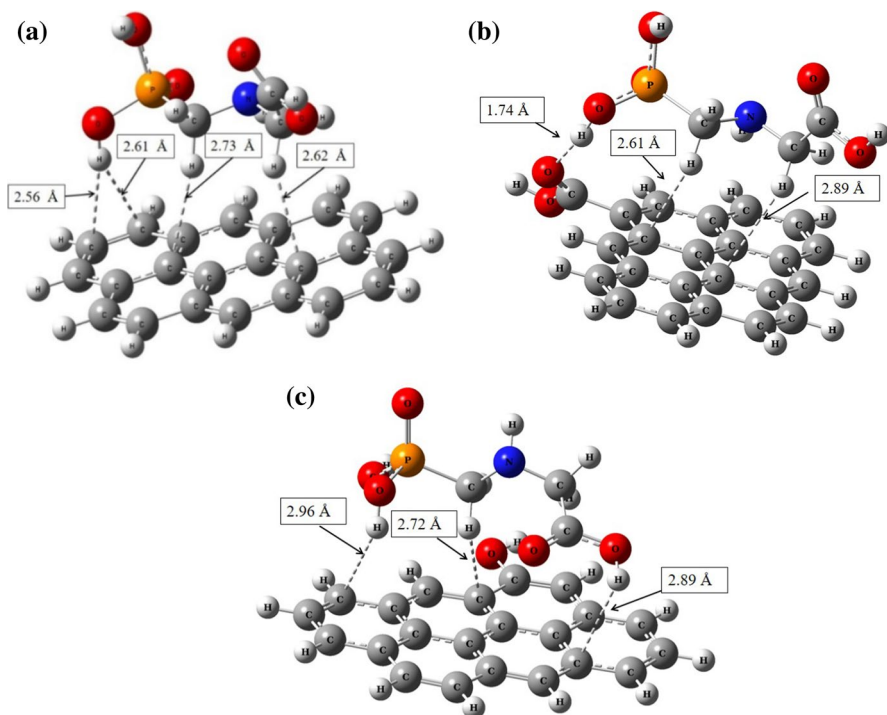
Fig. 5 Representation of the complexes formed between the matrices of activated carbon with GLY and their respective interaction distances

Table 3 Electronic interaction energy (ΔE_{int}) at 0 K, enthalpy (ΔH) and Gibbs energy (ΔG) at 298 K for adsorption processes between GLY and activated carbon

Complex	ΔE_{int} kcal mol^{-1}	ΔH	ΔG
(a) AC-GLY[a]	−11.92	−11.52	1.70
(b) AC-GLY[b]	−14.39	−14.39	0.36
(c) AC-GLY[c]	−11.63	−11.67	3.58

"a", "b" and "c" interactions of Fig. 5

Conclusion

Herein, the MEP and FMOs were analyzed to identify the possible interaction sites between ME and CX with glyphosate.

The obtained parameters of the interaction distance and vibrational frequencies provided evidence on the number of interactions that occurred during the formation of complexes, bond lengths, and that the interaction occurs. The QTAIM analysis corroborated the results of the energy parameters, showing that ME and CX derivatives are excellent matrices for the adsorption process.

The results show that activated carbon interacts better with the terminal group –COOH. Thus, the theoretical studies demonstrated that the biopolymers ME and CX present favorable structural, energetic, and topological aspects for glyphosate adsorption.

References

1. Grossbard E, Atkinson DC (1985) The herbicide glyphosate. BUTTERWORTH
2. Turner D (1985) Effects on glyphosate performance of formulation, additives and mixing with other herbicides, The Herbicide Glyphosate.
3. Tsui MTK, Chu LM (2003) Aquatic toxicity of glyphosate-based formulations: comparison between different organisms and the effects of environmental factors. Chemosphere 52:1189–1197. https://doi.org/10.1016/S0045-6535(03)00306-0
4. Richmond ME (2018) Glyphosate: A review of its global use, environmental impact, and potential health effects on humans and other species. J Environ Stud Sci 8:416–434. https://doi.org/10.1007/s13412-018-0517-2
5. PubChem, Hazardous Substances Data Bank (HSDB) : 3432, (n.d.). https://pubchem.ncbi.nlm.nih.gov/source/hsdb/3432. Accessed 20 Jan 2021
6. Nandula VK (2010) Glyphosate Resistance in Crops and Weeds: History, Development, and Management. Wiley, New York
7. de Aguiar Filho SQ, Costa AMF, dos Santos Pereira AK et al (2021) Interaction of glyphosate in matrices of cellulose and diethylaminoethyl cellulose biopolymers: theoretical viewpoint of the adsorption process. J Mol Model 27:272. https://doi.org/10.1007/s00894-021-04894-y
8. Van Bruggen AHC, He MM, Shin K, Mai V, Jeong KC, Finckh MR, Morris JG (2018) Environmental and health effects of the herbicide glyphosate. Sci Total Environ 616–617:255–268. https://doi.org/10.1016/j.scitotenv.2017.10.309
9. Mañas F, Peralta L, Raviolo J, Ovando HG, Weyers A, Ugnia L, Cid MG, Larripa I, Gorla N (2009) Genotoxicity of glyphosate assessed by the comet assay and cytogenetic tests. Environ Toxicol Pharmacol 28:37–41. https://doi.org/10.1016/j.etap.2009.02.001
10. Thongprakaisang S, Thiantanawat A, Rangkadilok N, Suriyo T, Satayavivad J (2013) Glyphosate induces human breast cancer cells growth via estrogen receptors. Food Chem Toxicol 59:129–136. https://doi.org/10.1016/j.fct.2013.05.057
11. IARC Working Group on the Evaluation of Carcinogenic Risks to Humans, Some organophosphate insecticides and herbicides, 2017. http://www.ncbi.nlm.nih.gov/books/NBK436774/. Accessed October 10, 2020.
12. Kwiatkowska M, Reszka E, Woźniak K, Jabłońska E, Michałowicz J, Bukowska B (2017) DNA damage and methylation induced by glyphosate in human peripheral blood mononuclear cells (in vitro study). Food Chem Toxicol 105:93–98. https://doi.org/10.1016/j.fct.2017.03.051
13. Duforestel M, Nadaradjane A, Bougras-Cartron G, Briand J, Olivier C, Frenel J-S, Vallette FM, Lelièvre SA, Cartron P-F (2019) Glyphosate primes mammary cells for tumorigenesis by reprogramming the epigenome in a TET3-dependent manner. Front Genet 10. https://doi.org/10.3389/fgene.2019.00885.

14. Castiglioni S, Bagnati R, Fanelli R, Pomati F, Calamari D, Zuccato E (2006) Removal of pharmaceuticals in sewage treatment plants in Italy. Environ Sci Technol 40:357–363. https://doi.org/10.1021/es050991m

15. Choy KKH, McKay G, Porter JF (1999) Sorption of acid dyes from effluents using activated carbon. Resources Conserv Recycling 27:57–71. https://doi.org/10.1016/S0921-3449(98)00085-8

16. Yagub MT, Sen TK, Afroze S, Ang HM (2014) Dye and its removal from aqueous solution by adsorption: a review. Adv Colloid Interface Sci 209:172–184. https://doi.org/10.1016/j.cis.2014.04.002

17. Madhav S, Ahamad A, Singh P, Mishra PK (2018) A review of textile industry: wet processing, environmental impacts, and effluent treatment methods. Environ Qual Manage 27:31–41. https://doi.org/10.1002/tqem.21538

18. Myers JP, Antoniou MN, Blumberg B, Carroll L, Colborn T, Everett LG, Hansen M, Landrigan PJ, Lanphear BP, Mesnage R, Vandenberg LN, vom Saal FS, Welshons WV, Benbrook CM (2016) Concerns over use of glyphosate-based herbicides and risks associated with exposures: a consensus statement. Environ Health 15:19. https://doi.org/10.1186/s12940-016-0117-0

19. Feng D, Malleret L, Soric A, Boutin O (2020) Kinetic study of glyphosate degradation in wet air oxidation conditions. Chemosphere 247:125930. https://doi.org/10.1016/j.chemosphere.2020.125930

20. Wang S, Peng Y (2010) Natural zeolites as effective adsorbents in water and wastewater treatment. Chem Eng J 156:11–24. https://doi.org/10.1016/j.cej.2009.10.029

21. Resende RF, Leal PVB, Pereira DH, Papini RM, Magriotis ZM (2020) Removal of fatty acid by natural and modified bentonites: elucidation of adsorption mechanism. Colloids Surfaces A Physicochem Eng Aspects 605:125340. https://doi.org/10.1016/j.colsurfa.2020.125340

22. Hameed BH, Krishni RR, Sata SA (2009) A novel agricultural waste adsorbent for the removal of cationic dye from aqueous solutions. J Hazard Mater 162:305–311. https://doi.org/10.1016/j.jhazmat.2008.05.036

23. Dai Y, Sun Q, Wang W, Lu L, Liu M, Li J, Yang S, Sun Y, Zhang K, Xu J, Zheng W, Hu Z, Yang Y, Gao Y, Chen Y, Zhang X, Gao F, Zhang Y (2018) Utilizations of agricultural waste as adsorbent for the removal of contaminants: a review. Chemosphere 211:235–253. https://doi.org/10.1016/j.chemosphere.2018.06.179

24. Geethakarthi A, Phanikumar BR (2010) Industrial sludge based adsorbents/ industrial by-products in the removal of reactive dyes A review. IJWREE 3:1–9. https://doi.org/10.5897/IJWREE.9000029

25. Ribeiro IHS, Reis DT, Pereira DH (2019) A DFT-based analysis of adsorption of Cd^{2+}, Cr^{3+}, Cu^{2+}, Hg^{2+}, Pb^{2+}, and Zn^{2+}, on vanillin monomer: a study of the removal of metal ions from effluents. J Mol Model 25:267. https://doi.org/10.1007/s00894-019-4151-z

26. Reis DT, Ribeiro IHS, Pereira DH (2020) DFT study of the application of polymers cellulose and cellulose acetate for adsorption of metal ions (Cd2+, Cu2+ and Cr3+) potentially toxic. Polym Bull 77:3443–3456. https://doi.org/10.1007/s00289-019-02926-5

27. Menazea AA, Ezzat HA, Omara W, Basyouni OH, Ibrahim SA, Mohamed AA, Tawfik W, Ibrahim MA (2020) Chitosan/graphene oxide composite as an effective removal of Ni, Cu, As, Cd and Pb from wastewater. Comput Theor Chem 1189:112980. https://doi.org/10.1016/j.comptc.2020.112980

28. Zhou S, Sun X, Jiang G (2021) A DFT study on the adsorption of nucleobases with Au20. J Mol Model 27:29. https://doi.org/10.1007/s00894-020-04618-8

29. Hohenberg P, Kohn W (1964) Inhomogeneous electron gas. Phys Rev 136:B864–B871. https://doi.org/10.1103/PhysRev.136.B864

30. Kohn W, Sham LJ (1965) Self-consistent equations including exchange and correlation effects. Phys Rev 140:A1133–A1138. https://doi.org/10.1103/PhysRev.140.A1133

31. Parr RG, Yang W (1989) Density functional theory of atoms and molecules, vol 1. OXford University Press, Oxford, p 989.

32. Becke AD (2014) Perspective: fifty years of density-functional theory in chemical physics. J Chem Phys 140:18A301. https://doi.org/10.1063/1.4869598

33. Chai J-D, Head-Gordon M (2008) Long-range corrected hybrid density functionals with damped atom–atom dispersion corrections. Phys Chem Chem Phys 10:6615–6620. https://doi.org/10.1039/B810189B

34. Ditchfield R, Hehre WJ, Pople JA (1971) Self-consistent molecular-orbital methods. IX. An extended Gaussian-type basis for molecular-orbital studies of organic molecules. J Chem Phys 54:724–728. https://doi.org/10.1063/1.1674902

35. Hehre WJ, Ditchfield R, Pople JA (1972) Self—Consistent molecular orbital methods. XII. Further extensions of Gaussian—type basis sets for use in molecular orbital studies of organic molecules. J Chem Phys 56:2257–2261. https://doi.org/10.1063/1.1677527.

36. Hariharan PC, Pople JA (1973) The influence of polarization functions on molecular orbital hydrogenation energies. Theoret Chim Acta 28:213–222. https://doi.org/10.1007/BF00533485

37. Marenich AV, Cramer CJ, Truhlar DG (2009) Universal Solvation model based on solute electron density and on a continuum model of the solvent defined by the bulk dielectric constant and atomic surface tensions. J Phys Chem B 113:6378–6396. https://doi.org/10.1021/jp810292n

38. Dennington R, Keith T, Millam JG (2009) Gauss View, Version 5; Semichem Inc: Shawnee Mission

39. Frisch J, Trucks GW, Schlegel HB, Scuseria GE, Robb MA, Cheeseman JR, Scalmani G, Barone V, Mennucci B, Petersson GA, Nakatsuji H, Caricato M, Li X, Hratchian HP, Izmaylov AF, Bloino J, Zheng G, Sonnenberg JL, Hada M, Ehara M, Toyota K, Fukuda R, Hasegawa J, Ishida M, Nakajima T, Honda Y, Kitao O, Nakai H, Vreven T, Montgomery JA, Peralta JE, Ogliaro F, Bearpark M, Heyd JJ, Brothers E, Kudin KN, Staroverov VN, Kobayashi R, Normand J, Raghavachari K, Rendell A, Burant JC, Iyengar SS, Tomasi J, Cossi M, Rega N, Millam JM, Klene M, Knox JE, Cross JB, Bakken V, Adamo C, Jaramillo J, Gomperts R, Stratmann RE, Yazyev O, Austin AJ, Cammi R, Pomelli C, Ochterski JW, Martin RL, Morokuma K, Zakrzewski VG, Voth GA, Salvador P, Dannenberg JJ, Dapprich S, Daniels AD, Farkas Ö, Foresman JB, Ortiz JV, Cioslowski J, Fox DJ (2009) Gaussian09, Revision D.01, Gaussian, Inc., Wallingford.

40. Bader RFW, Essén H (1984) The characterization of atomic interactions. J Chem Phys 80:1943–1960. https://doi.org/10.1063/1.446956

41. Bader RFW (1990) Atoms in molecules: a quantum theory, 1st edn. Oxford University Press, Oxford

42. Keith TA, Bader RFW, Aray Y (1996) Structural homeomorphism between the electron density and the virial field. Int J Quantum Chem 57:183–198. https://doi.org/10.1002/(SICI)1097-461X(1996)57:2%3c183::AID-QUA4%3e3.0.CO;2-U

43. Popelier PLA (1999) Quantum Molecular Similarity. 1. BCP Space. J Phys Chem A 103:2883–2890. https://doi.org/10.1021/jp984735q.

44. Todd A, Keith T (2017) AIMAll (Version 10.05. 04), Gristmill Software, Overland Park KS, USA

45. Mohamed Naseer Ali M, Kaliannan P, Venuvanalingam P (2005) Conformation and function of N-hydroxy-glyphosate and N-amino-glyphosate: a comparative study using ab initio MO theory. J Molecular Structure THEOCHEM 714(2005):99–108. https://doi.org/10.1016/j.theochem.2004.10.026

46. Kaliannan P, Mohamed Naseer Ali M, Seethalakshmi T, Venuvanalingam P (2002) Electronic structure and conformation of glyphosate: an ab initio MO study. J Molecular Structure THEOCHEM. 618:117–125. https://doi.org/10.1016/S0166-1280(02)00467-0.

47. Costa MPM, Prates LM, Baptista L, Cruz MTM, Ferreira ILM (2018) Interaction of polyelectrolyte complex between sodium alginate and chitosan dimers with a single glyphosate molecule: A DFT and NBO study. Carbohyd Polym 198:51–60. https://doi.org/10.1016/j.carbpol.2018.06.052

48. Ahmed AA, Gros P, Kühn O, Leinweber P (2018) Molecular level investigation of the role of peptide interactions in the glyphosate analytics. Chemosphere 196:129–134. https://doi.org/10.1016/j.chemosphere.2017.12.162

49. Costa AMF, de Aguiar Filho SQ, Santos TJ, Pereira DH (2021) Theoretical insights about the possibility of removing Pb2+ and Hg2+ metal ions using adsorptive processes and matrices of carboxymethyl diethylaminoethyl cellulose and cellulose nitrate biopolymers. J Molecular Liquids. 331:115730. https://doi.org/10.1016/j.molliq.2021.115730.

50. Sprankle P, Meggitt WF, Penner D (1975) Adsorption, mobility, and microbial degradation of glyphosate in the soil. Weed Sci 23:229–234

51. Reis DT, Pereira AKS, Scheidt GN, Pereira DH (2019) Plant and bacterial cellulose: production, chemical structure, derivatives and applications, orbital. Electronic J Chem 11:321–329. https://doi.org/10.17807/orbital.v11i5.1349

52. Reis DT, de Aguiar Filho SQ, Grotto CGL, Bihain MFR, Pereira DH (2020) Carboxymethylcellulose and cellulose xanthate matrices as potential adsorbent material for potentially toxic Cr3+, Cu2+ and Cd2+ metal ions: a theoretical study. Theor Chem Acc 139:96. https://doi.org/10.1007/s00214-020-02610-2.

53. Melchor-Rodríguez K, Gaspard S, Jáuregui-Haza U (2020) Chlordecone adsorption on functionalized activated carbons: computational chemistry as tool for understanding the adsorption process. Quím. Nova. https://doi.org/10.21577/0100-4042.20170666.

54. Carneiro RTA, Taketa TB, Gomes Neto RJ, Oliveira JL, Campos EVR, de Moraes MA, da Silva CMG, Beppu MM, Fraceto LF (2015) Removal of glyphosate herbicide from water using biopolymer membranes. J Environ Manae 151:353–360. https://doi.org/10.1016/j.jenvman.2015.01.005.
55. Moradeeya PG, Kumar MA, Thorat RB, Rathod M, Khambhaty Y, Basha S (2017) Nanocellulose for biosorption of chlorpyrifos from water: chemometric optimization, kinetics and equilibrium. Cellulose 24:1319–1332. https://doi.org/10.1007/s10570-017-1197-x
56. Rissouli l, Benicha M, Chafik T, Chabbi D (2017) Decontamination of water polluted with pesticide using biopolymers: adsorption of glyphosate by chitin and chitosan. JMES 8:4544–4549. https://doi.org/10.26872/jmes.2017.8.12.479.
57. Desbrières J, Guibal E (2018) Chitosan for wastewater treatment: Chitosan for wastewater treatment. Polym Int 67:7–14. https://doi.org/10.1002/pi.5464
58. Sanchez LM, Ollier RP, Pereira AES, Fraceto L, Alvarez VA (2020) Pesticide removal from industrial effluents using biopolymeric materials. In: Biopolymer Membranes and Films. Elsevier, Amsterdam, pp 359–382

Publisher's Note Springer Nature remains neutral with regard to jurisdictional claims in published maps and institutional affiliations.

Authors and Affiliations

Sílvio Quintino de Aguiar Filho[1] · Anna Karla dos Santos Pereira[2] · Grasiele Soares Cavallini[1] · Douglas Henrique Pereira[1]

1   Chemistry Collegiate, Federal University of Tocantins, Campus Gurupi - Badejós, P.O. Box 66, Gurupi 77 402-970, Tocantins, Brazil

2   Institute of Chemistry, University of Campinas – UNICAMP, P.O. Box 6154, Campinas, SP 13083-970, Brazil